Supplementary Data

Medial prefrontal cortex–pontine nuclei projections modulate suboptimal cue induced associative motor learning

Guang-Yan Wu[1,2,*], Shu-Lei Liu[1,2,*], Juan Yao[2], Lin Sun[3], Bing Wu[2], Yi Yang[2], Xuan Li[2], Qian-Quan Sun[4], Hua Feng[5] and Jian-Feng Sui[1,2]

[1]Department of Physiology, College of Basic Medical Sciences, Third Military Medical University, Chongqing 400038, China;

[2]Experimental Center of Basic Medicine, College of Basic Medical Sciences, Third Military Medical University, Chongqing 400038, China;

[3]Institute of Physical Education, Southwest University, Chongqing, 400715, China;

[4]Department of Zoology and Physiology, University of Wyoming, Laramie, WY 82071, USA;

[5]Department of Neurosurgery, Southwest Hospital, Third Military Medical University, Chongqing 400038, China.

[*]These authors contributed equally to this work.

Address correspondence to Jian-feng Sui, Email: jfsui2003@163.com; Hua Feng, Email: fenghua8888@vip.163.com.

Supplementary Figures

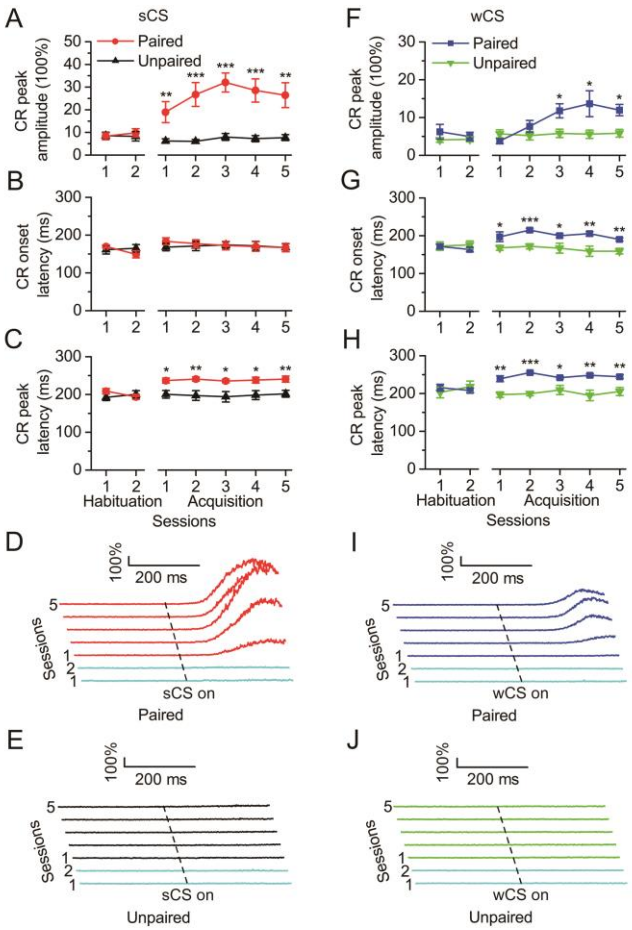

Supplementary Figure 1. The peak amplitude (*A*,*F*), onset latency (*B*,*G*), and peak latency (*C*,*H*) of CR and EMG response topographies (*D*,*E*,*I*,*J*) in DEC with the sCS or wCS, respectively, across two habituation and five acquisition sessions (related to Fig. 1*C*,*E*; N.S., not significant, **P*< 0.05, ***P*< 0.01,****P*< 0.001; two-way ANOVA with repeated measures followed by Tukey post-hoc test). The EMG amplitude is given as a percentage of the baseline (100%) averaged EMG amplitude. Data are represented as mean ± s.e.m.

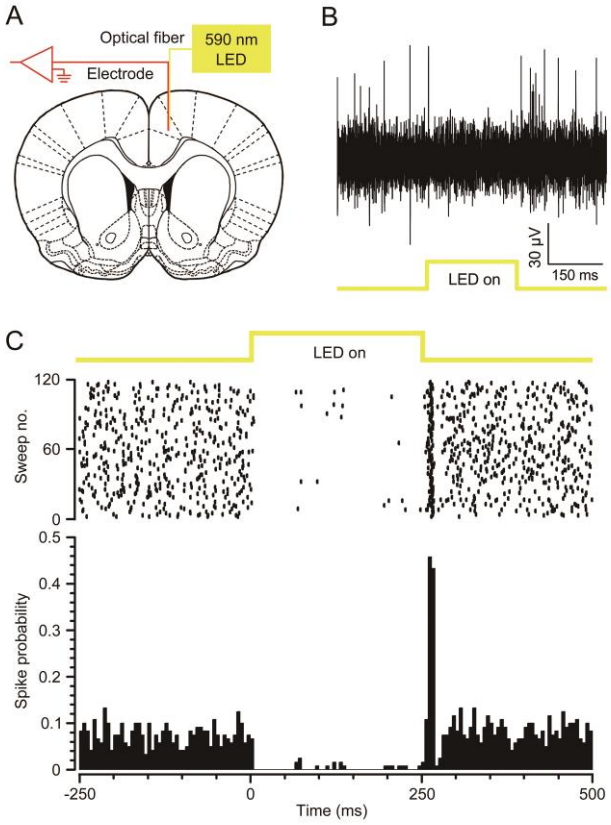

Supplementary Figure 2. 590-nmLED illumination suppressed eNpHR3.0-EYFP-expressing cells in the right caudal mPFC. (*A*) Schematic of *in vivo* optogenetic inhibition and recording in the right caudal mPFC. (*B*,*C*) Continuous 590-nm LED illumination (250 ms, 15 mW/mm^2) of the mPFC expressing eNpHR3.0-EYFP in anesthetized rats inhibited neuronal firing in a temporally precise, stable, and reversible manner.

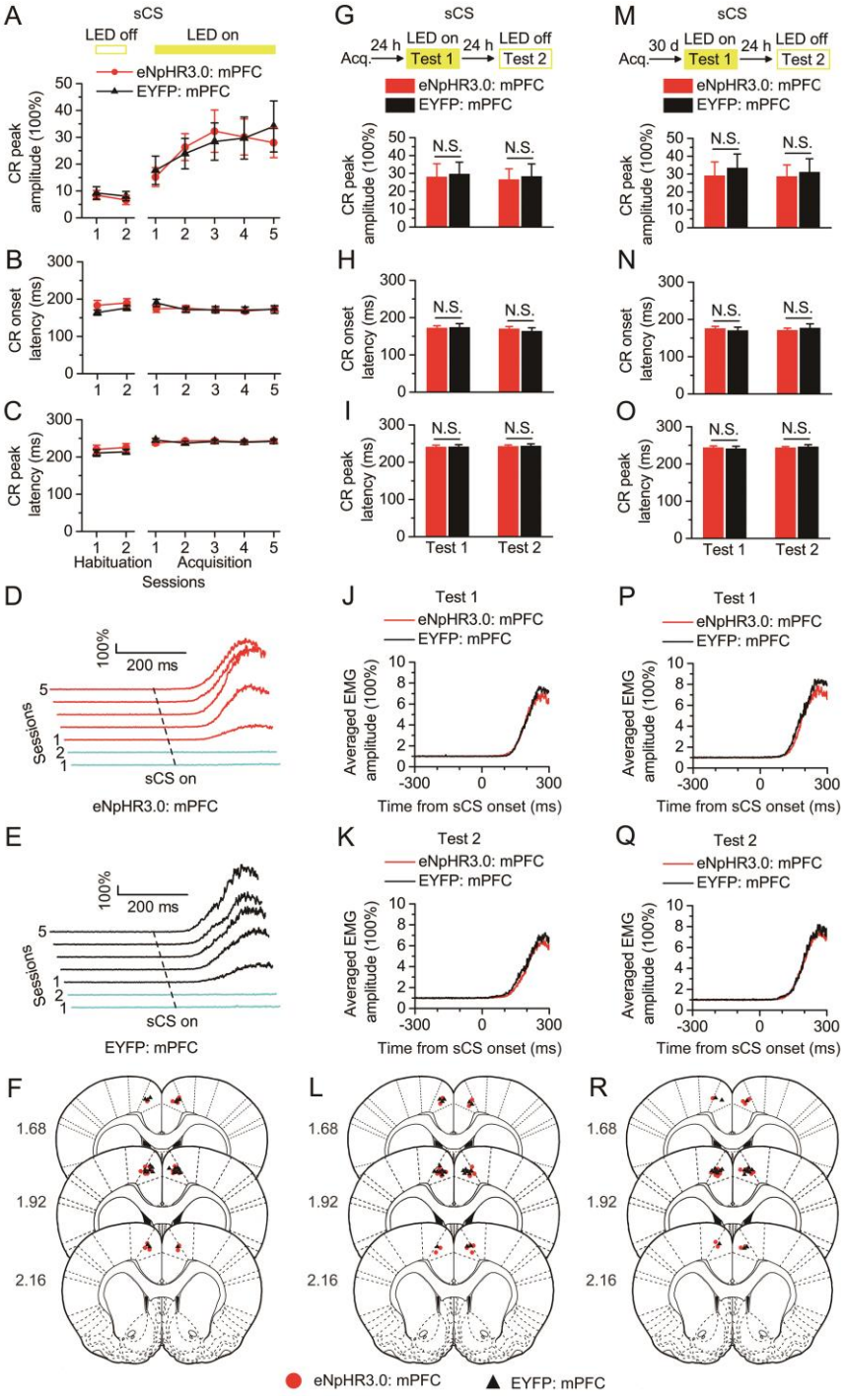

Supplementary Figure 3. Effects of optogenetic inhibition of the bilateral caudal mPFC on the peak amplitude, onset latency, and peak latency of CR with the sCS (related to Fig. 2*F–H*). (*A–C*) Top: Training and illumination protocol. Bottom: Optogenetic inhibition of the bilateral caudal mPFC during acquisition training failed to impair the peak amplitude (*A*), onset latency (*B*), or peak latency (*C*) of CR with the sCS (two-way ANOVA with repeated measures). (*D*,*E*) The EMG response topographies of eNpHR3.0: mPFC (*D*) and EYFP: mPFC (*E*) groups were shown across

two habituation and five acquisition sessions. (*F*) Approximate locations of fiber optic cannula tips for optogenetic inhibition experiment (related to Fig. 2*F*) among rats of eNpHR3.0: mPFC and EYFP: mPFC groups. Numbers indicate the anteroposterior coordinates from bregma. (*G–I*) Top: Training and illumination protocol. Rats were eyeblink conditioned in the absence of optogenetic inhibition and tested 24 h later. Bottom: Twenty-four hours after the acquisition training, optogenetic inhibition of the bilateral caudal mPFC did not affect the peak amplitude (*G*), onset latency (*H*), or peak latency (*I*) of CR with the sCS (N.S., not significant; two-tailed unpaired Student's t-test). (*J,K*) The EMG response topographies for eNpHR3.0: mPFC and EYFP: mPFC groups during test 1 (*J*) and test 2 (*K*) were shown. (*L*) Same as (*F*), except rats from the other optogenetic inhibition experimen (related to Fig. 2*G*). (*M–R*) Same as (*G–L*), except the optogenetic inhibition was applied at thirty days after the acquisition training (related to Fig. 2*H*; N.S., not significant; two-tailed unpaired Student's t-test). The EMG amplitude is given as a percentage of the baseline (100%) averaged EMG amplitude. Data are represented as mean ± s.e.m.

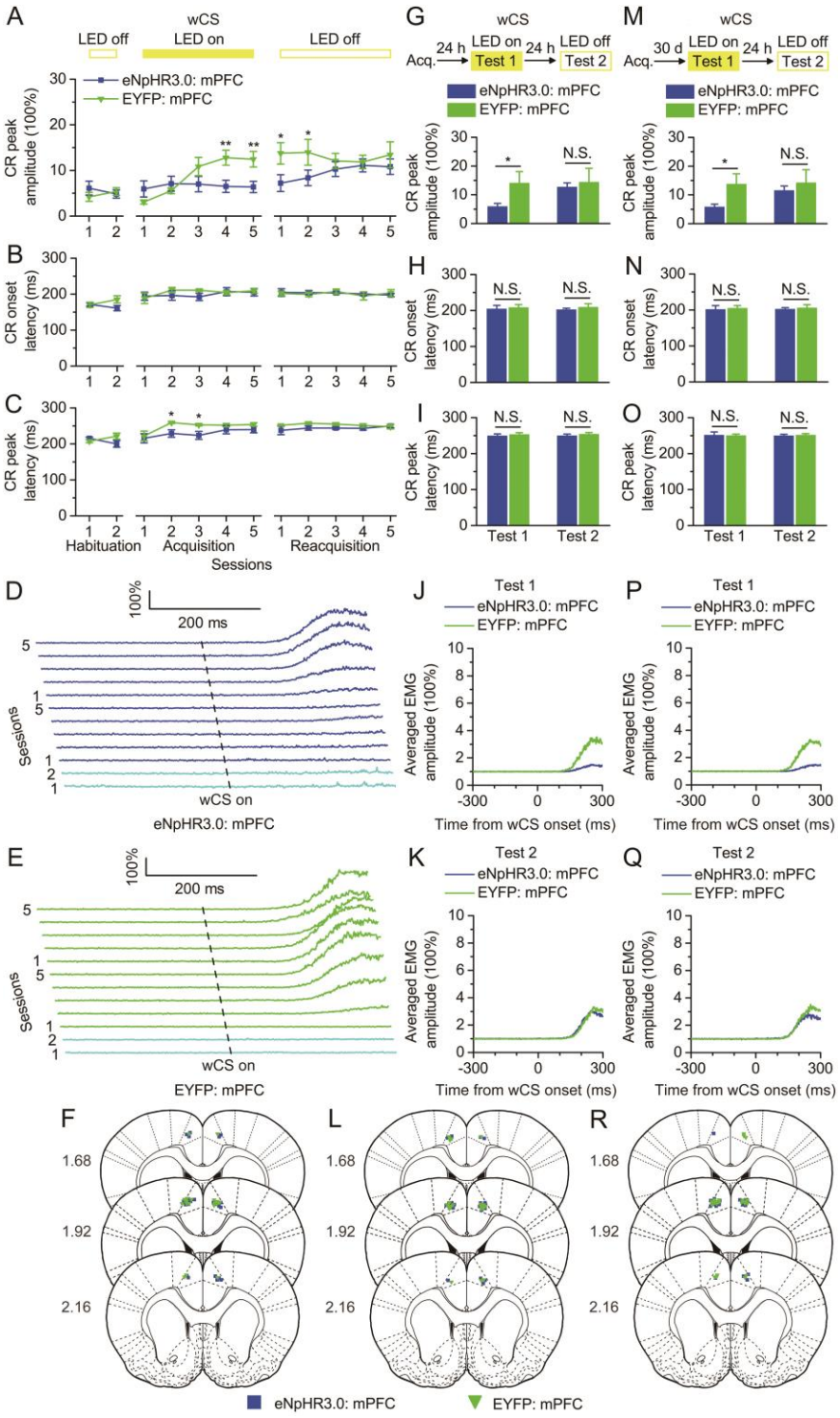

Supplementary Figure 4. Effects of optogenetic inhibition of the bilateral caudal mPFC on the peak amplitude, onset latency, and peak latency of CR with the wCS (related to Fig. 2*I–K*). (*A–C*) Top: Training and illumination protocol. Bottom: Optogenetic inhibition of the bilateral caudal mPFC during acquisition training affected the peak amplitude (*A*) and peak latency (*C*), but not onset latency (*B*) of CR with the wCS (*P< 0.05, **P< 0.01; two-way ANOVA with repeated

measures followed by Tukey post-hoc test). (*D*,*E*) The EMG response topographies of eNpHR3.0: mPFC (*D*) and EYFP: mPFC (*E*) groups were shown across two habituation, five acquisition, and five reacquisition sessions. (*F*) Approximate locations of fiber optic cannula tips for optogenetic inhibition experiment (related to Fig. 2*I*) among rats of eNpHR3.0: mPFC and EYFP: mPFC groups. Numbers indicate the anteroposterior coordinates from bregma. (*G*–*I*) Top: Training and illumination protocol. Rats were eyeblink conditioned in the absence of optogenetic inhibition and tested 24 h later. Bottom: Twenty-four hours after the acquisition training, optogenetic inhibition of the bilateral caudal mPFC affected the peak amplitude (*G*), but not onset latency (*H*) or peak latency (*I*) of CR with the sCS (N.S., not significant, **P*< 0.05; two-tailed unpaired Student's t-test). (*J*,*K*) The EMG response topographies for eNpHR3.0: mPFC and EYFP: mPFC groups during test 1 (*J*) and test 2 (*K*) were shown. (*L*) Same as (*F*), except rats from the other optogenetic inhibition experiment (related to Fig. 2*J*). (*M*–*R*) Same as (*G*–*L*), except the optogenetic inhibition was applied at thirty days after the acquisition training (related to Fig. 2*K*; N.S., not significant, **P*< 0.05; two-tailed unpaired Student's t-test). The EMG amplitude is given as a percentage of the baseline (100%) averaged EMG amplitude. Data are represented as mean ± s.e.m.

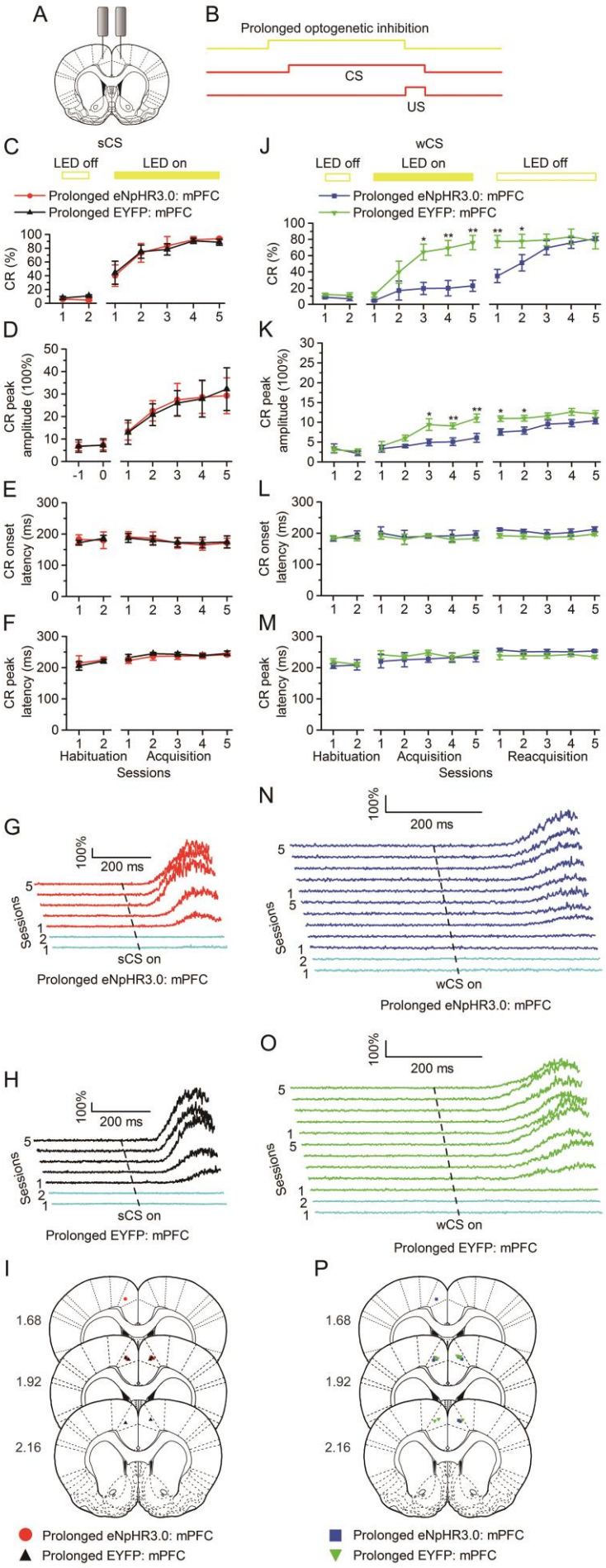
A
B
Prolonged optogenetic inhibition
CS
US
C
sCS
LED off
LED on
Prolonged eNpHR3.0: mPFC
Prolonged EYFP: mPFC
CR (%)
D
CR peak amplitude (100%)
E
CR onset latency (ms)
F
CR peak latency (ms)
Habituation
Acquisition
Sessions
J
wCS
LED off
LED on
LED off
Prolonged eNpHR3.0: mPFC
Prolonged EYFP: mPFC
CR (%)
K
CR peak amplitude (100%)
L
CR onset latency (ms)
M
CR peak latency (ms)
Habituation
Acquisition
Reacquisition
Sessions
G
100%
200 ms
Sessions
sCS on
Prolonged eNpHR3.0: mPFC
N
100%
200 ms
Sessions
wCS on
Prolonged eNpHR3.0: mPFC
H
100%
200 ms
Sessions
sCS on
Prolonged EYFP: mPFC
O
100%
200 ms
Sessions
wCS on
Prolonged EYFP: mPFC
I
1.68
1.92
2.16
Prolonged eNpHR3.0: mPFC
Prolonged EYFP: mPFC
P
1.68
1.92
2.16
Prolonged eNpHR3.0: mPFC
Prolonged EYFP: mPFC

Supplementary Figure 5. Effects of prolonged optogenetic inhibition of the bilateral caudal mPFC on the percentage, peak amplitude, onset latency, and peak latency of CR with the sCS or wCS. (*A*,*B*) Scheme for optical fiber implant site and 590-nm LED illumination pattern to bilateral caudal mPFC during each trial. (*C*–*F*) Top: Training and illumination phase protocol. Bottom: Prolonged optogenetic inhibition of the bilateral caudal mPFC during acquisition training did not affect the percentage (*C*), peak amplitude (*D*), onset latency (*E*), or peak latency (*F*) of CR with the sCS (n = 3 each; two-way ANOVA with repeated measures). (*G*,*H*) The EMG response topographies of Prolonged eNpHR3.0: mPFC (*G*) and Prolonged EYFP: mPFC (*H*) groups with sCS were shown across two habituation and five acquisition sessions. (*I*) Approximate locations of fiber optic cannula tips for Prolonged optogenetic inhibition experiment with sCS (related to *C*–*H*) among rats of Prolonged eNpHR3.0: mPFC and Prolonged EYFP: mPFC groups. Numbers indicate the anteroposterior coordinates from bregma. (*J*–*M*) Top: Training and illumination phase protocol. Bottom: Prolonged optogenetic inhibition of the bilateral caudal mPFC during acquisition training significantly impaired the percentage (*J*) and peak amplitude (*K*), but not peak latency (*L*) or onset latency (*M*) of CR with the wCS (n = 4 each; $^{*}P < 0.05$, $^{**}P < 0.01$; two-way ANOVA with repeated measures followed by Tukey post-hoc test). (*N*,*O*) The EMG response topographies of Prolonged eNpHR3.0: mPFC (*N*) and Prolonged EYFP: mPFC (*O*) groups with wCS were shown across two habituation, five acquisition, and five reacquisition sessions. (*P*) Same as (*I*), except rats from the Prolonged optogenetic inhibition experiment with wCS (related to *J*–*O*). The EMG amplitude is given as a percentage of the baseline (100%) averaged EMG amplitude. Data are represented as mean ± s.e.m.

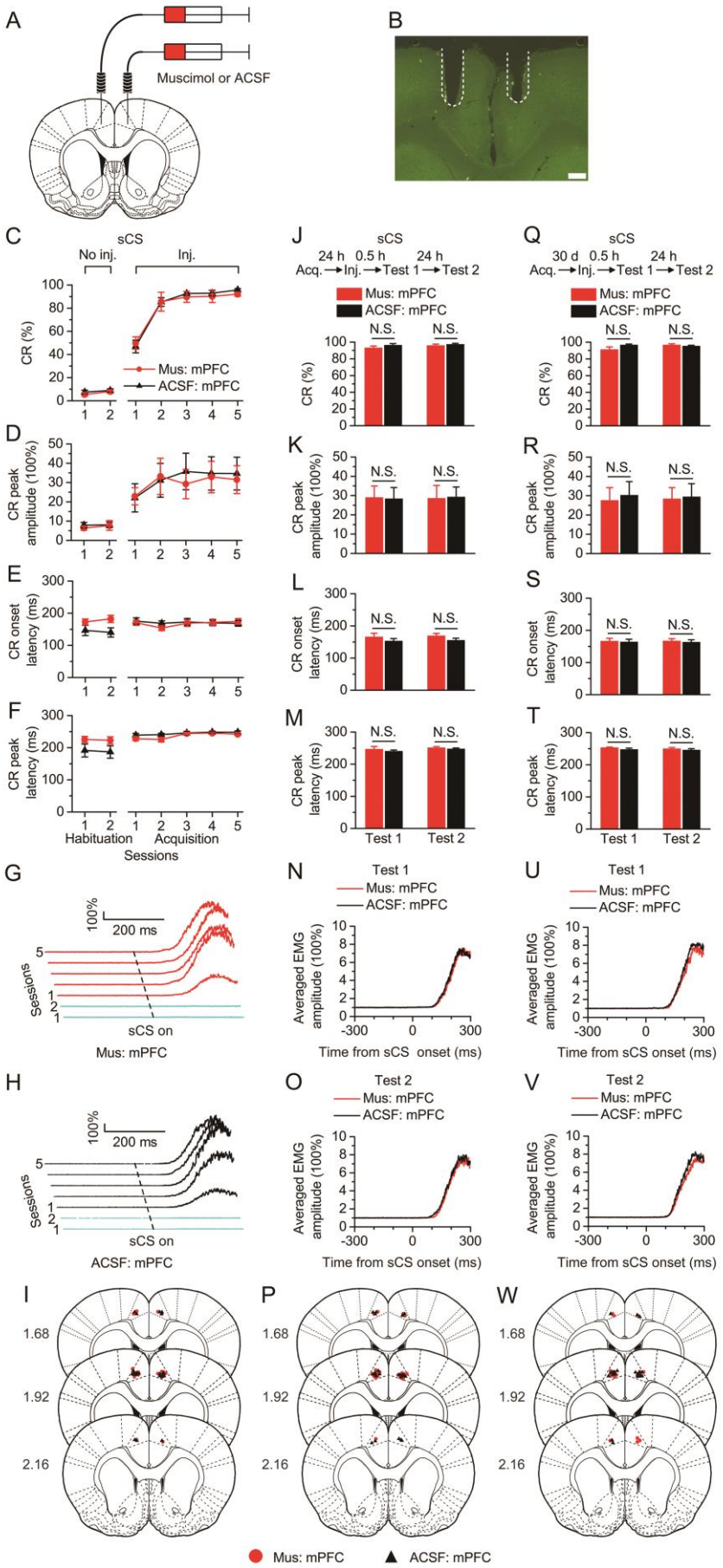

Supplementary Figure 6. Effects of muscimol inactivation of the bilateral caudal mPFC on the

percentage, peak amplitude, onset latency, and peak latency of CR with the sCS. (*A*) Schematic of *in vivo* muscimol or ACSF injection into the bilateral caudal. (*B*) Representative image showing locations of infusion cannula tips in the bilateral caudal. (*C–F*) Top: Training and infusion protocol. Bottom: Muscimol inactivation of the bilateral caudal mPFC during acquisition training did not affect the percentage (*C*), peak amplitude (*D*), onset latency (*E*), or peak latency (*F*) of CR with the sCS (n = 11 each; two-way ANOVA with repeated measures). (*G*,*H*) The EMG response topographies of Mus: mPFC (*G*) and ACSF: mPFC (*H*) groups were shown across two habituation and five acquisition sessions. (*I*) Approximate locations of infusion cannula tips for muscimol inactivation experiment (related to *C–H*) among rats of Mus: mPFC and ACSF: mPFC groups. Numbers indicate the anteroposterior coordinates from bregma. (*J–M*) Top: Training and infusion protocol. Rats were eyeblink conditioned in the absence of muscimol and tested 24 h later. Bottom: Twenty-four hours after the acquisition training, muscimol inactivation of the bilateral caudal mPFC did not affect the percentage (*J*), peak amplitude (*K*), onset latency (*L*), or peak latency (*M*) of CR with the sCS (n = 11 each; N.S., not significant; two-tailed unpaired Student's t-test). (*N*,*O*) The EMG response topographies for Mus: mPFC and ACSF: mPFC groups during test 1 (*N*) and test 2 (*O*) were shown. (*P*) Same as (*I*), except rats from the other muscimol inactivation experiment (related to *J–O*). (*Q–W*) Same as (*I–P*), except the muscimol inactivation was applied at thirty days after the acquisition training (n = 11 Mus: mPFC, n = 10 ACSF: mPFC groups; N.S., not significant; two-tailed unpaired Student's t-test). The EMG amplitude is given as a percentage of the baseline (100%) averaged EMG amplitude. Data are represented as mean ± s.e.m.

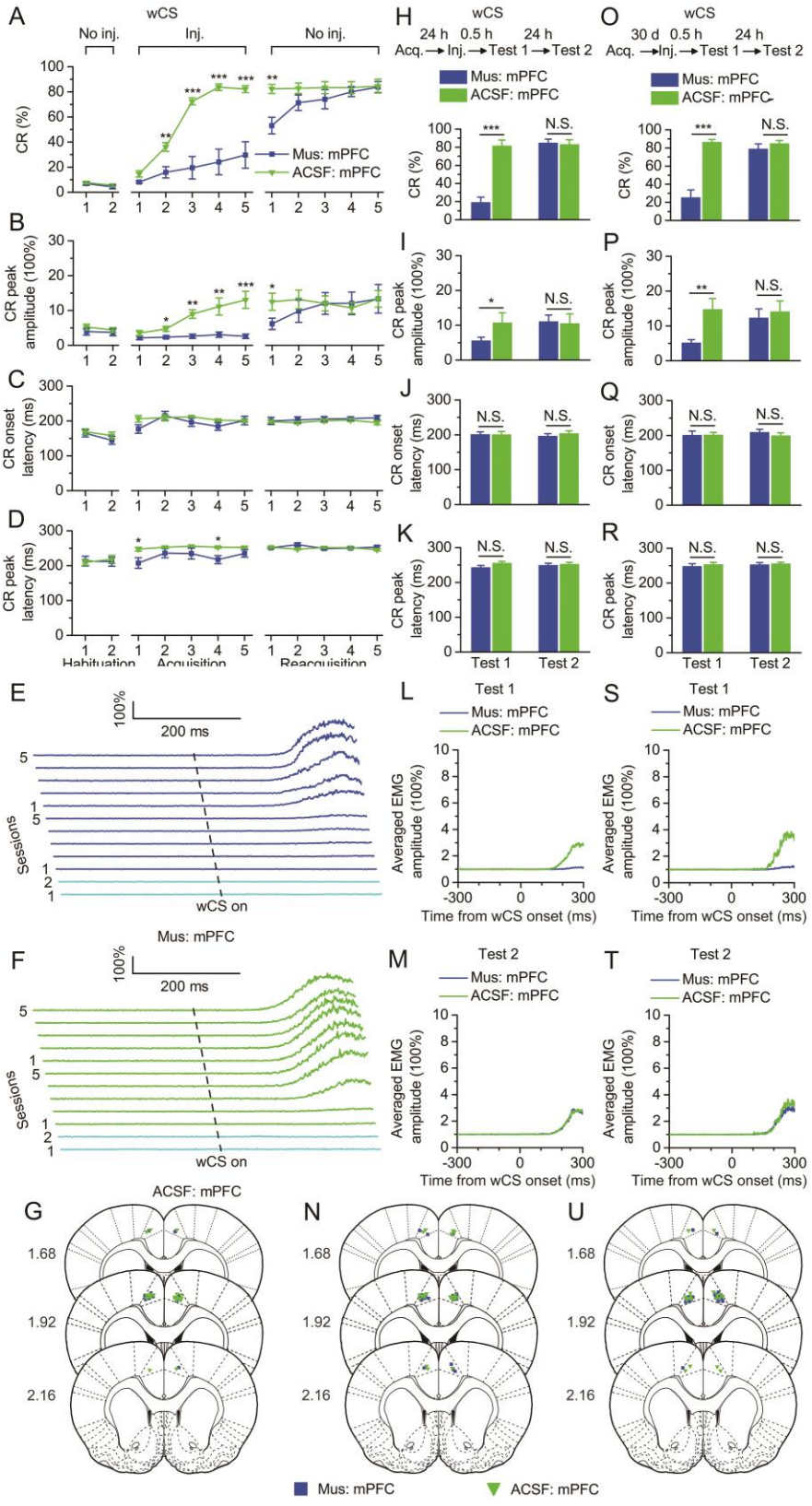

Supplementary Figure 7. Effects of muscimol inactivation of the bilateral caudal mPFC on the percentage, peak amplitude, onset latency, and peak latency of CR with the wCS. (*A–D*) Top: Training and infusion protocol. Bottom: Muscimol inactivation of the bilateral caudal mPFC during

acquisition training significantly affected the percentage (*A*), peak amplitude (*B*), and peak latency (*D*), but not onset latency (*C*) of CR with the wCS (*n* = 8 Mus: mPFC, *n* = 10 ACSF: mPFC; **P*< 0.05, ***P*< 0.01, ****P*< 0.001; two-way ANOVA with repeated measures followed by Tukey post-hoc test). (*E*, *F*) The EMG response topographies of Mus: mPFC (*E*) and ACSF: mPFC (*F*) groups were shown across two habituation, five acquisition, and five reacquisition sessions. (*G*) Approximate locations of infusion cannula tips for muscimol inactivation experiment (related to *A*–*F*) among rats of Mus: mPFC and ACSF: mPFC groups. Numbers indicate the anteroposterior coordinates from bregma. (*H–K*) Top: Training and infusion protocol. Rats were eyeblink conditioned in the absence of muscimol and tested 24 h later. Bottom: Twenty-four hours after the acquisition training, muscimol inactivation of the bilateral caudal mPFC substantially affected the percentage (*H*) and peak amplitude (*I*), but not onset latency (*J*) or peak latency (*K*) of CR with the wCS (*n* = 11 Mus: mPFC, *n* = 10 ACSF: mPFC; N.S., not significant, **P*< 0.05, ****P*< 0.001; two-tailed unpaired Student's t-test). (*L*,*M*) The EMG response topographies for Mus: mPFC and ACSF: mPFC groups during test 1 (*L*) and test 2 (*M*) were shown. (*N*) Same as (*G*), except rats from the other muscimol inactivation experiment (related to *H–M*). (*O–U*) Same as (*H–N*), except the muscimol inactivationwas applied at thirty days after the acquisition training (*n* = 10 subjects for Mus: mPFC, and *n* = 9 subjects for ACSF: mPFC groups; N.S., not significant, ***P*< 0.01, ****P*< 0.001; two-tailed unpaired Student's t-test). The EMG amplitude is given as a percentage of the baseline (100%) averaged EMG amplitude. Data are represented as mean ± s.e.m.

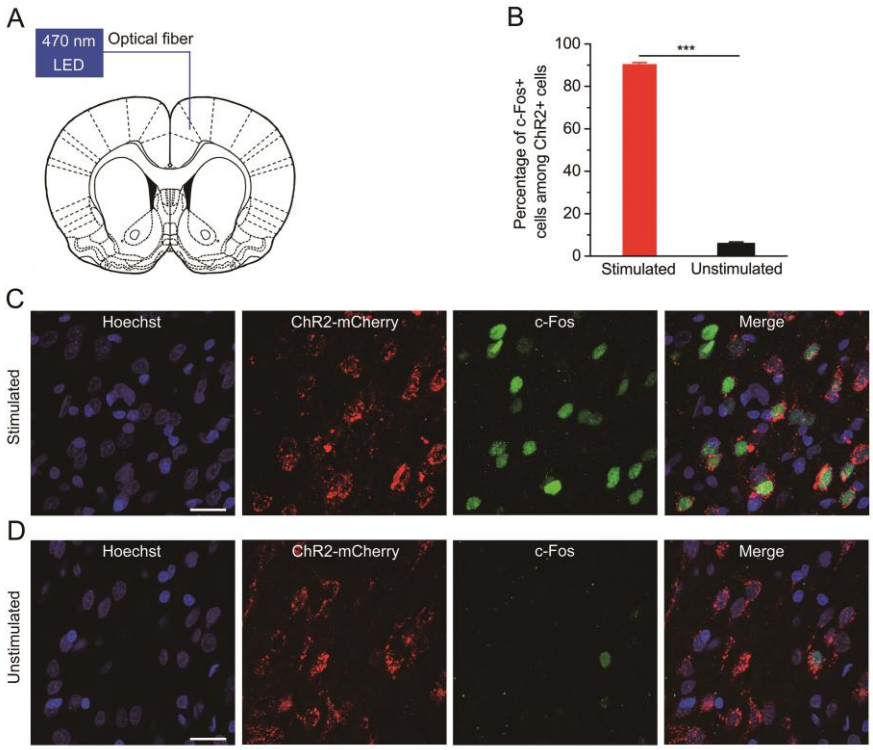

Supplementary Figure 8. 470-nm LED stimulation induced c-Fos expression in cells expressing ChR2-mCherry in the mPFC. (*A*) Schematic diagram of optical stimulation of ChR2-mCherry-expressing cells in right caudal mPFC. (*B–D*) Rats expressing ChR2-mCherry (red) in the mPFC were treated with or without 470-nm LED stimulation and the expression of c-Fos (green) was examined. Representative magnification images of mPFC for the light stimulated group (*C*) and unstimulated group (*D*) are shown. Scale bar, 20 μm. Quantification of c-Fos positive cells among ChR2 positive cells is shown in (*B*).

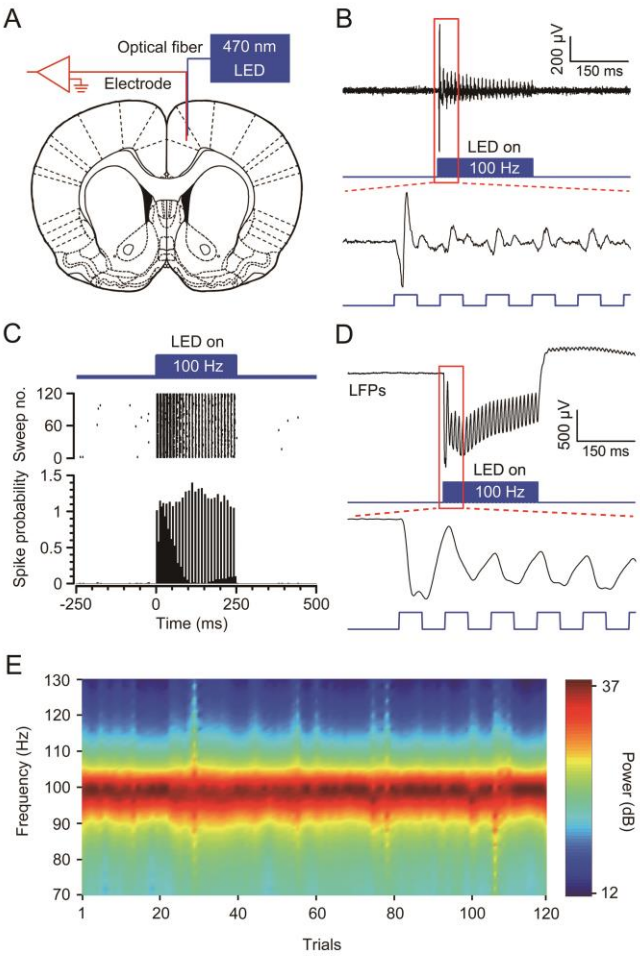

Supplementary Figure 9. 470-nm LED illumination evoked activation of ChR2-mCherry-expressing cells in the right caudal mPFC. (*A*) Schematic showing *in vivo* optical stimulation and recording in the right caudal mPFC. (*B*,*C*) Trains of 25 light pulses (470 nm, 15 mW/mm^2, 100 Hz, 5 ms pulse duration) induced reliable spikes in the right caudal mPFC neurons recorded from head-fixed anesthetized rats injected with pAAV 2/9-CaMKIIα-ChR2-mCherry. (*D*,*E*) Trains of 25 light pulses (470 nm, 15 mW/mm^2, 100 Hz, 5 ms pulse duration) also evoked robust LFP responses in right caudal mPFC in awake behaving rats. Note that the (*D*) graph illustrates an example of the mean value of 120 light-induced LFPs.

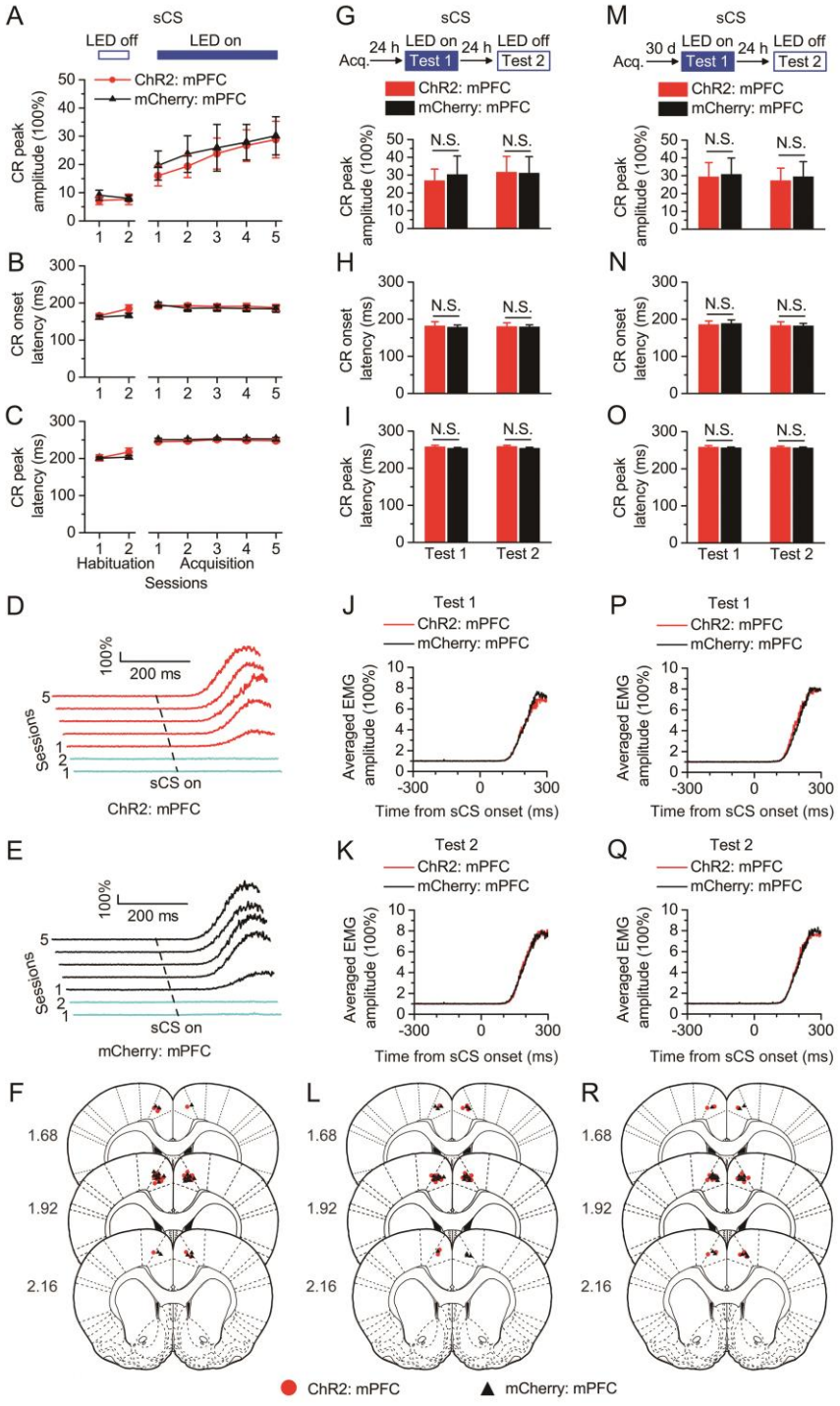

Supplementary Figure 10. Effects of optogenetic activation of the bilateral caudal mPFC on the peak amplitude, onset latency, and peak latency of CR with the sCS (related to Fig. 3*F–H*). (*A–C*) Top: Training and illumination protocol. Bottom: Optogenetic activation of the bilateral caudal mPFC during acquisition training failed to affect the peak amplitude (*A*), onset latency (*B*), or peak latency (*C*) of CR with the sCS (two-way ANOVA with repeated measures). (*D*,*E*) The EMG response topographies of ChR2: mPFC (*D*) and mCherry: mPFC (*E*) groups were shown across two

habituation and five acquisition sessions. (*F*) Approximate locations of optrode tips for optogenetic activation experiment (related to Fig. 3*F*) among rats of ChR2: mPFC and mCherry: mPFC groups. Numbers indicate the anteroposterior coordinates from bregma. (*G–I*) Top: Training and illumination protocol. Rats were eyeblink conditioned in the absence of optogenetic activation and tested 24 h later. Bottom: Twenty-four hours after the acquisition training, optogenetic activation of the bilateral caudal mPFC did not affect the peak amplitude (*G*), onset latency (*H*), or peak latency (*I*) of CR with the sCS (N.S., not significant; two-tailed unpaired Student's t-test). (*J*,*K*) The EMG response topographies for ChR2: mPFC and mCherry: mPFC groups during test 1 (*J*) and test 2 (*K*) were shown. (*L*) Same as (*F*), except rats from the other optogenetic activation experiment (related to Fig. 3*G*). (*M–R*) Same as (*G–L*), except the optogenetic activation was applied at thirty days after the acquisition training (related to Fig. 3*H*; N.S., not significant; two-tailed unpaired Student's t-test). The EMG amplitude is given as a percentage of the baseline (100%) averaged EMG amplitude. Data are represented as mean ± s.e.m.

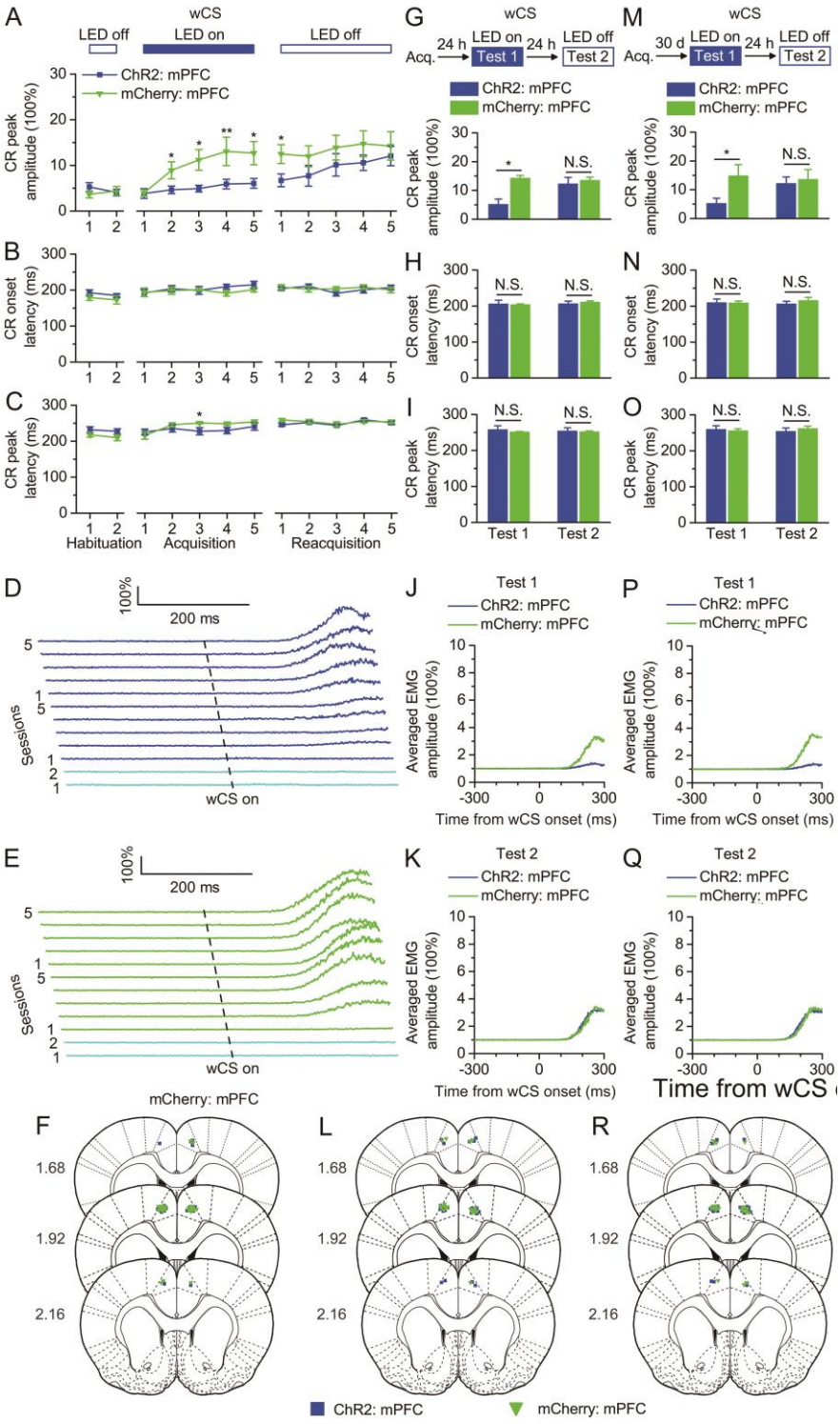

Supplementary Figure 11. Effects of optogenetic activation of the bilateral caudal mPFC on the peak amplitude, onset latency, and peak latency of CR with the wCS (related to Fig. 3*I–K*). (*A–C*) Top: Training and illumination protocol. Bottom: Optogenetic activation of the bilateral caudal mPFC during acquisition training affected the peak amplitude (*A*) and peak latency (*C*), but not onset latency (*B*) of CR with the wCS (*P< 0.05, **P< 0.01; two-way ANOVA with repeated

measures followed by Tukey post-hoc test). (*D*,*E*) The EMG response topographies of ChR2: mPFC (*D*) and mCherry: mPFC (*E*) groups were shown across two habituation, five acquisition, and five reacquisition sessions. (*F*) Approximate locations of optrode tips for optogenetic activation experiment (related to Fig. 3*I*) among rats of ChR2: mPFC and mCherry: mPFC groups. Numbers indicate the anteroposterior coordinates from bregma. (*G–I*) Top: Training and illumination protocol. Rats were eyeblink conditioned in the absence of optogenetic activation and tested 24 h later. Bottom: Twenty-four hours after the acquisition training, optogenetic activation of the bilateral caudal mPFC affected the peak amplitude (*G*), but not onset latency (*H*) or peak latency (*I*) of CR with the sCS (N.S., not significant, **P*< 0.05; two-tailed unpaired Student's t-test). (*J*,*K*) The EMG response topographies for ChR2: mPFC and mCherry: mPFC groups during test 1 (*J*) and test 2 (*K*) were shown. (*L*) Same as (*F*), except rats from the other optogenetic activation experiment (related to Fig. 3*J*). (*M–R*) Same as (*G–L*), except the optogenetic activation was applied at thirty days after the acquisition training (related to Fig. 3*K*; N.S., not significant, **P*< 0.05; two-tailed unpaired Student's t-test). The EMG amplitude is given as a percentage of the baseline (100%) averaged EMG amplitude. Data are represented as mean ± s.e.m.

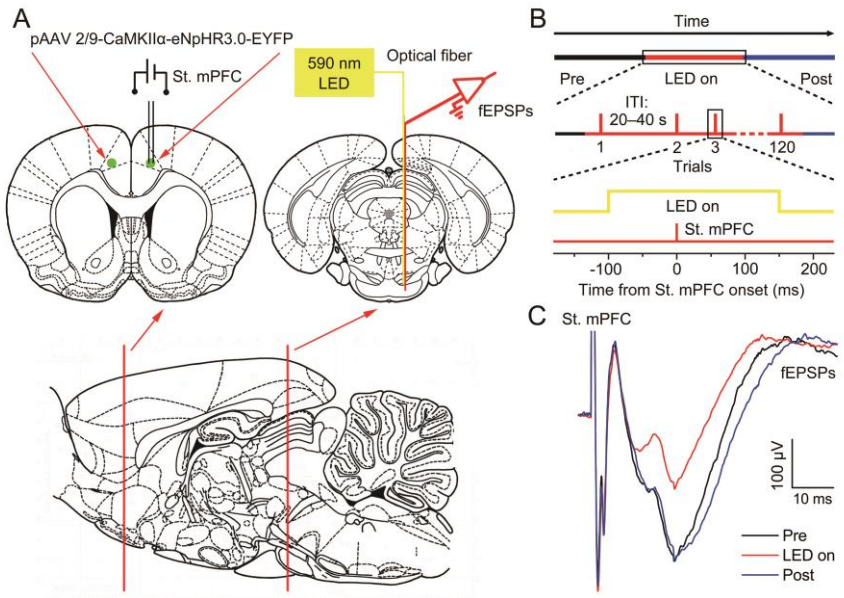

Supplementary Figure 12. 590-nm LED illumination of eNpHR3.0-EYFP-expressing mPFC axon terminals in the right PN significantly decreased the slope of fEPSPs evoked by the electrical stimulation of the right caudal mPFC. (*A*) Schematic depicting a concentric stimulating electrode and an optrode implanted in vivo for stimulating neurons in the right caudal mPFC, optogenetic inhibition of mPFC axon terminals in the right PN, and for recording in fEPSPs in the right PN, respectively. (*B*) Time line for examination of the effect of optogenetic inhibition on fEPSPs. Top: The full experiment was divided into three epochs, i.e., pre epoch, LED on epoch, and post LED on epoch. Middle: Each epoch consisted of 120 trials, separated by a variable interval of 20–40 s. Bottom: Only during LED on epoch, the continuous 590-nm illumination (25 mW/mm^2) was delivered 100 ms before electrical stimulation of the right caudal mPFC and lasted 250 ms. (*C*) The slope of the fEPSPs evoked at the right caudal mPFC was significantly decreased by optogenetic illumination of the caudal mPFC axon terminals in the right PN.

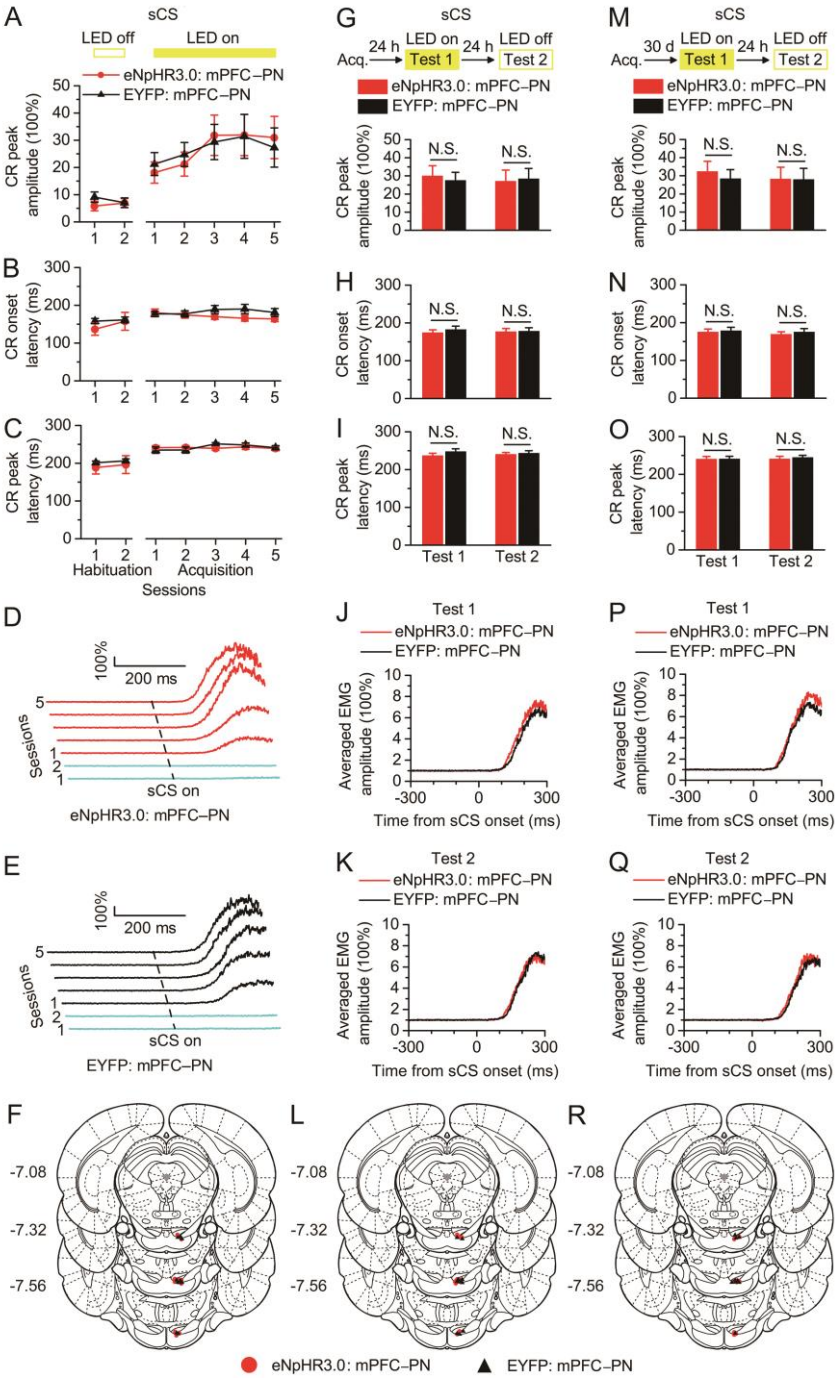

Supplementary Figure 13. Effects of optogenetic inhibition of the caudal mPFC axon terminals in the right PN on the peak amplitude, onset latency, and peak latency of CR with the sCS (related to Fig. 4*E*–*G*). (*A*–*C*) Top: Training and illumination protocol. Bottom: Optogenetic inhibition of the caudal mPFC axon terminals in the right PN during acquisition training failed to impair the peak amplitude (*A*), onset latency (*B*), or peak latency (*C*) of CR with the sCS (two-way ANOVA with repeated measures). (*D*,*E*) The EMG response topographies of eNpHR3.0: mPFC–PN (*D*) and

EYFP: mPFC–PN (*E*) groups were shown across two habituation and five acquisition sessions. (*F*) Approximate locations of fiber optic cannula tips for optogenetic inhibition experiment (related to Fig. 4*E*) among rats of eNpHR3.0: mPFC–PN and EYFP: mPFC–PN groups. Numbers indicate the anteroposterior coordinates from bregma. (*G–I*) Top: Training and illumination protocol. Rats were eyeblink conditioned in the absence of optogenetic inhibition and tested 24 h later. Bottom: Twenty-four hours after the acquisition training, optogenetic inhibition of the caudal mPFC axon terminals in the right PN did not affect the peak amplitude (*G*), onset latency (*H*), or peak latency (*I*) of CR with the sCS (N.S., not significant; two-tailed unpaired Student's t-test). (*J*,*K*) The EMG response topographies for eNpHR3.0: mPFC–PN and EYFP: mPFC–PN groups during test 1 (*J*) and test 2 (*K*) were shown. (*L*) Same as (*F*), except rats from the other optogenetic inhibition experiment (related to Fig. 4*F*). (*M–R*) Same as (*G–L*), except the optogenetic inhibition was applied at thirty days after the acquisition training (related to Fig. 4*G*; N.S., not significant; two-tailed unpaired Student's t-test). The EMG amplitude is given as a percentage of the baseline (100%) averaged EMG amplitude. Data are represented as mean ± s.e.m.

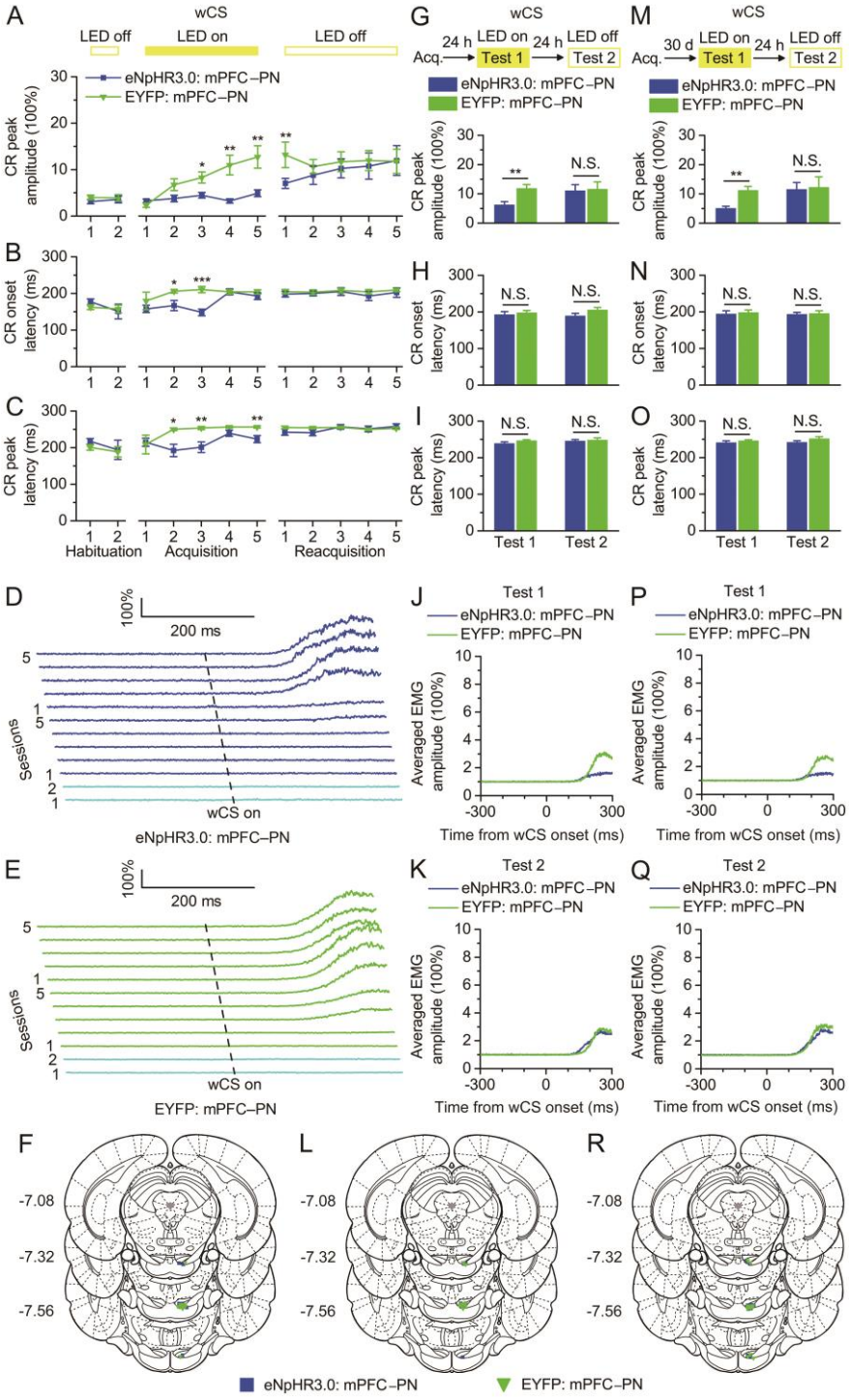

241

242 **Supplementary Figure 14.** Effects of optogenetic inhibition of the caudal mPFC axon terminals in

243 the right PN on the peak amplitude, onset latency, and peak latency of CR with the wCS (related to

244 Fig. 4*H–J*). (*A-C*) Top: Training and illumination protocol. Bottom: Optogenetic inhibition of the

245 caudal mPFC axon terminals in the right PN during acquisition training affected the peak amplitude

246 (*A*), onset latency (*B*), and peak latency (*C*) of CR with the wCS (**P*< 0.05, ***P*< 0.01, ****P*<

247 0.001; two-way ANOVA with repeated measures followed by Tukey post-hoc test). (*D,E*) The

EMG response topographies of eNpHR3.0: mPFC–PN (*D*) and EYFP: mPFC–PN (*E*) groups were shown across two habituation, five acquisition, and five reacquisition sessions. (*F*) Approximate locations of fiber optic cannula tips for optogenetic inhibition experiment (related to Fig. 4*H*) among rats of eNpHR3.0: mPFC–PN and EYFP: mPFC–PN groups. Numbers indicate the anteroposterior coordinates from bregma. (*G–I*) Top: Training and illumination protocol. Rats were eyeblink conditioned in the absence of optogenetic inhibition and tested 24 h later. Bottom: Twenty-four hours after the acquisition training, optogenetic inhibition of the bilateral caudal mPFC affected the peak amplitude (*G*), but not onset latency (*H*) or peak latency (*I*) of CR with the sCS (N.S., not significant, $^{**}P < 0.01$; two-tailed unpaired Student's t-test). (*J*,*K*) The EMG response topographies for eNpHR3.0: mPFC–PN and EYFP: mPFC–PN groups during test 1 (*J*) and test 2 (*K*) were shown. (*L*) Same as (*F*), except rats from the other optogenetic inhibition experiment (related to Fig. 4*I*). (*M–R*) Same as (*G–L*), except the optogenetic inhibition was applied at thirty days after the acquisition training (related to Fig. 4*J*; N.S., not significant, $^{**}P < 0.01$; two-tailed unpaired Student's t-test). The EMG amplitude is given as a percentage of the baseline (100%) averaged EMG amplitude. Data are represented as mean ± s.e.m.

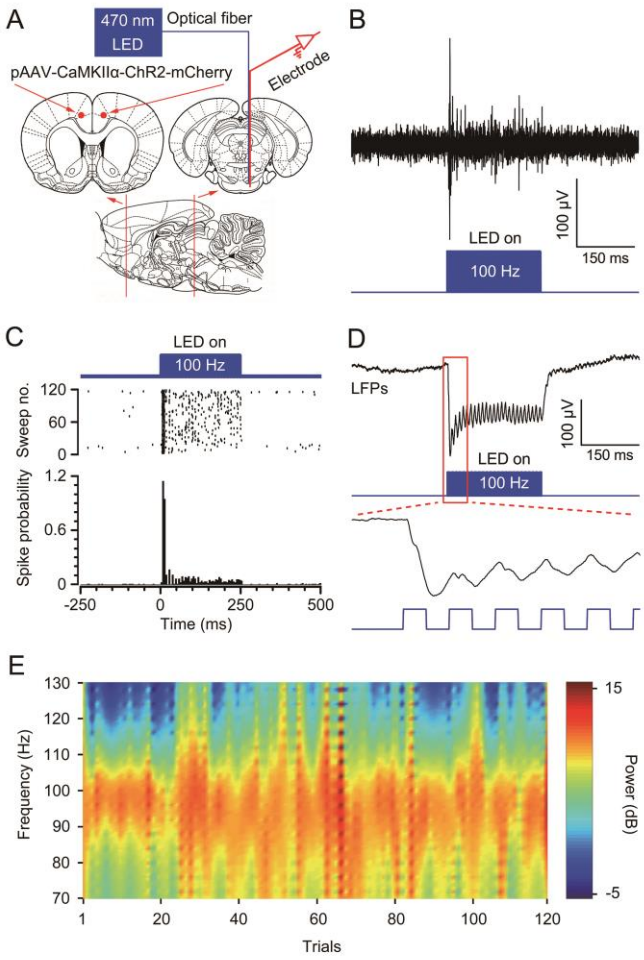

Supplementary Figure 15. 470-nm LED illumination of the axon terminals of ChR2-mCherry-expressing caudal mPFC neurons in the PN evoked activation of the right PN. (*A*) Schematic illustration of *in vivo* optical stimulation and recording in the right PN. (*B*,*C*) Local spikes in the right PN were induced by trains of 25 light pulses (470 nm, 25 mW/mm^2, 100 Hz, 5 ms pulse duration) to the caudal mPFC axon terminals in the right PN of head-fixed anesthetized rats injected with pAAV 2/9-CaMKIIα-ChR2-mCherry into the bilateral caudal mPFC. Note that the spikes were not elicited with every light pulse. (*D*,*E*) Trains of 25 light pulses (470 nm, 25 mW/mm^2, 100 Hz, 5 ms pulse duration) also evoked robust LFP responses in the right PN of a wake behaving rats. Note that the graph (*D*) illustrates an example of the mean value of 120 light-induced LFPs.

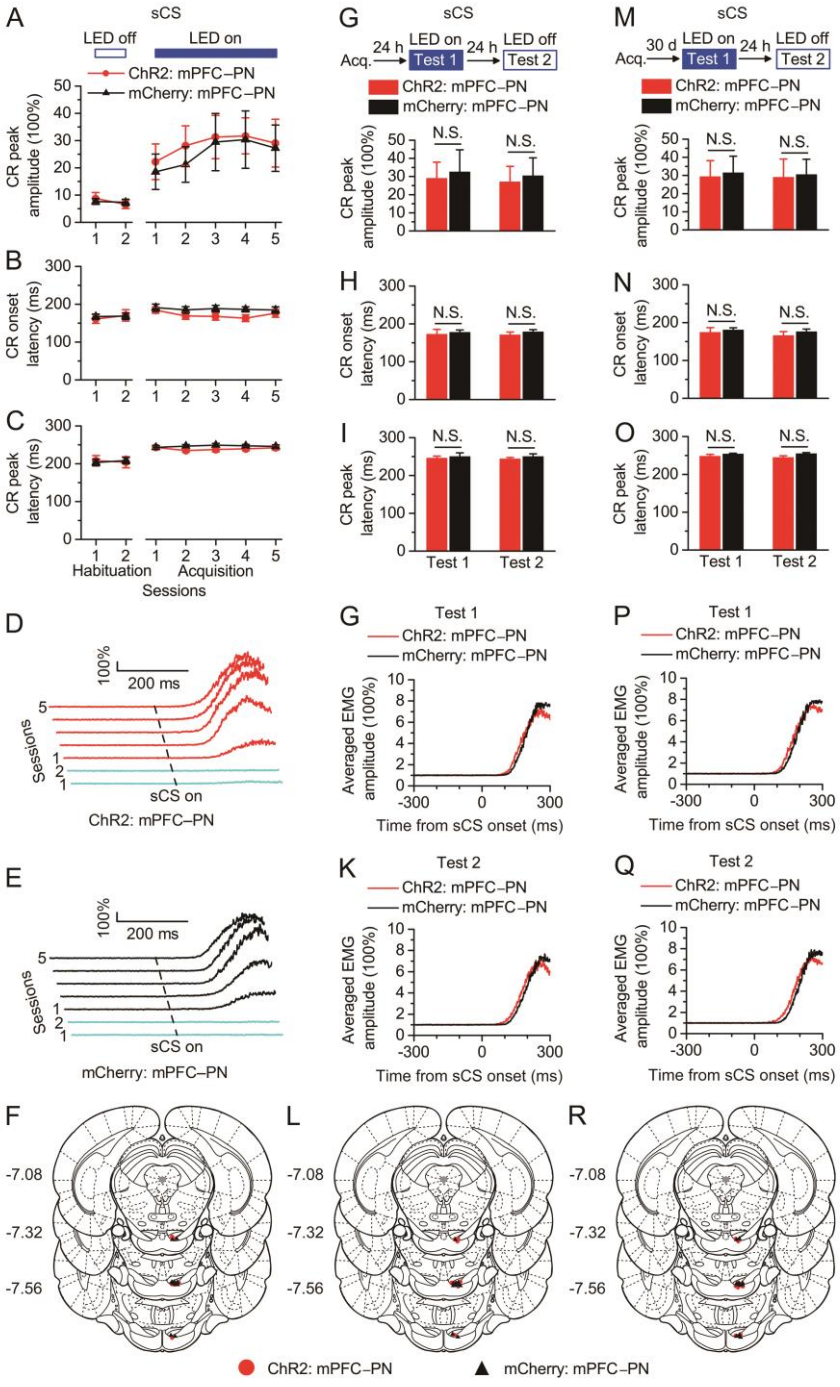

Supplementary Figure 16. Effects of optogenetic activation of the caudal mPFC axon terminals in the right PN on the peak amplitude, onset latency, and peak latency of CR with the sCS (related to Fig. 5*E–G*). (***A–C***) Top: Training and illumination protocol. Bottom: Optogenetic activation of the caudal mPFC axon terminals in the right PN during acquisition training also failed to produced deficits in the peak amplitude (***A***), onset latency (***B***), or peak latency (***C***) of CR with the sCS (two-way ANOVA with repeated measures). (***D***,***E***) The EMG response topographies of ChR2:

mPFC–PN (***D***) and mCherry: mPFC–PN (***E***) groups were shown across two habituation and five acquisition sessions. (***F***) Approximate locations of optrode tips for optogenetic activation experiment (related to Fig. 5*E*) among rats of ChR2: mPFC–PN and mCherry: mPFC–PN groups. Numbers indicate the anteroposterior coordinates from bregma. (***G–I***) Top: Training and illumination protocol. Rats were eyeblink conditioned in the absence of optogenetic activation and tested 24 h later. Bottom: Twenty-four hours after the acquisition training, optogenetic activation of the caudal mPFC axon terminals in the right PN also did not affect the peak amplitude (***G***), onset latency (***H***), or peak latency (***I***) of CR with the sCS (N.S., not significant; two-tailed unpaired Student's t-test). (***J***,***K***) The EMG response topographies for ChR2: mPFC–PN and mCherry: mPFC–PN groups during test 1 (***J***) and test 2 (***K***) were shown. (***L***) Same as (***F***), except rats from the other optogenetic activation experiment (related to Fig. 5*F*). (***M–R***) Same as (***G–L***), except the optogenetic activation was applied at thirty days after the acquisition training (related to Fig. 5*G*; N.S., not significant; two-tailed unpaired Student's t-test). The EMG amplitude is given as a percentage of the baseline (100%) averaged EMG amplitude. Data are represented as mean ± s.e.m.

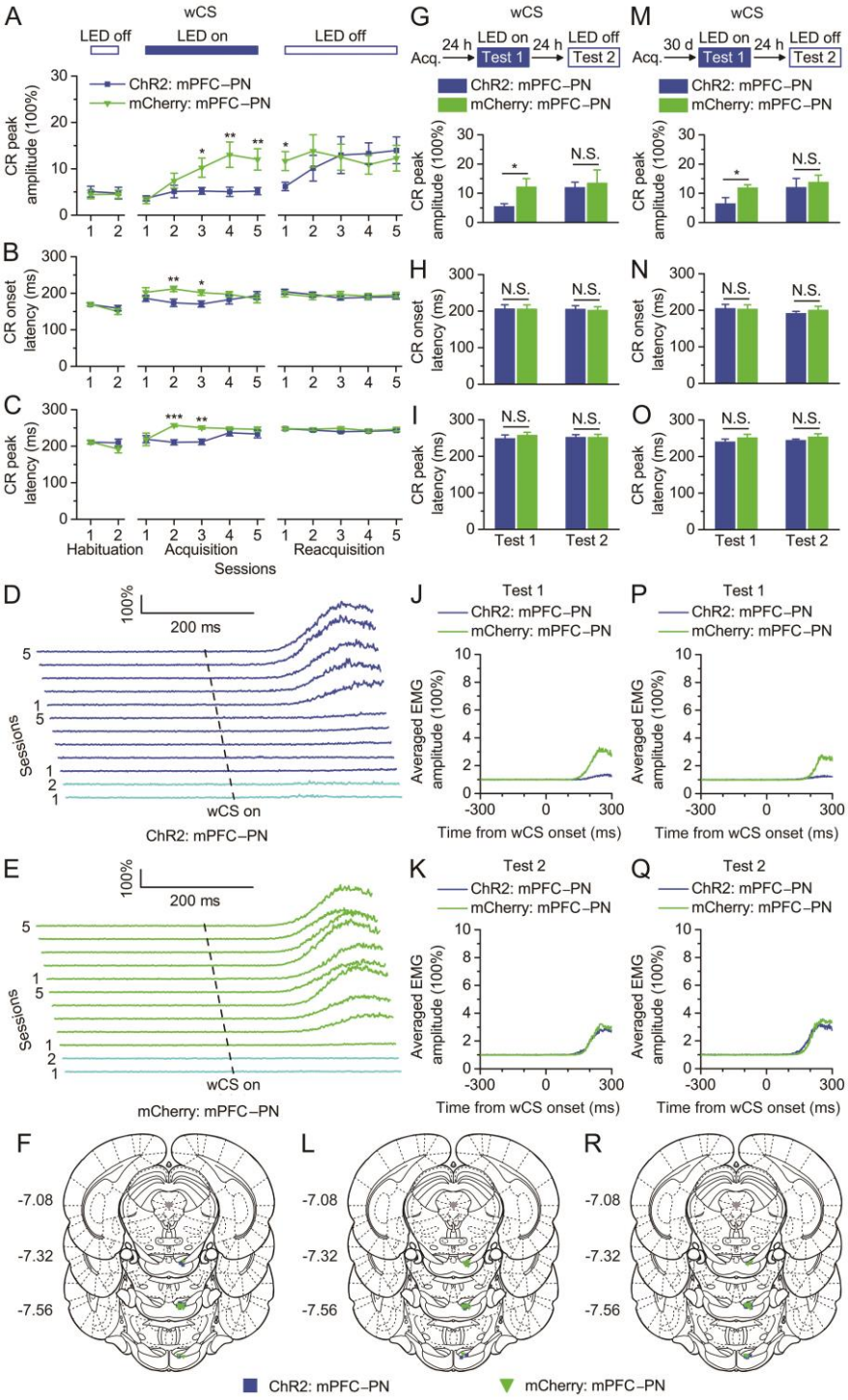

Supplementary Figure 17. Effects of optogenetic activation of the caudal mPFC axon terminals in the right PN on the peak amplitude, onset latency, and peak latency of CR with the wCS (related to Fig. 5*H–J*). (*A–C*) Top: Training and illumination protocol. Bottom: Optogenetic activation of the caudal mPFC axon terminals in the right PN during acquisition training produced significantly deficits in the peak amplitude (*A*), onset latency (*B*), and peak latency (*C*) of CR with the wCS (**P*< 0.05, ***P*< 0.01, ****P*< 0.001;two-way ANOVA with repeated measures followed by Tukey

post-hoc test). (*D*,*E*) The EMG response topographies of ChR2: mPFC–PN (*D*) and mCherry: mPFC–PN (*E*) groups were shown across two habituation, five acquisition, and five reacquisition sessions. (*F*) Approximate locations of optrode tips for optogenetic activation experiment (related to Fig. 5*H*) among rats of ChR2: mPFC–PN and mCherry: mPFC–PN groups. Numbers indicate the anteroposterior coordinates from bregma. (*G–I*) Top: Training and illumination protocol. Rats were eyeblink conditioned in the absence of optogenetic activation and tested 24 h later. Bottom: Twenty-four hours after the acquisition training, optogenetic activation of the caudal mPFC axon terminals in the right PN affected the peak amplitude (*G*), but not onset latency (*H*), or peak latency (*I*) of CR with the wCS (N.S., not significant, $*P < 0.05$; two-tailed unpaired Student's t-test). (*J*,*K*) The EMG response topographies for ChR2: mPFC–PN and mCherry: mPFC–PN groups during test 1 (*J*) and test 2 (*K*) were shown. (*L*) Same as (*F*), except rats from the other optogenetic activation experiment (related to Fig. 5*I*). (*M–R*) Same as (*G–L*), except the optogenetic activation was applied at thirty days after the acquisition training (related to Fig. 5*J*; N.S., not significant, $*P < 0.05$; two-tailed unpaired Student's t-test). The EMG amplitude is given as a percentage of the baseline (100%) averaged EMG amplitude. Data are represented as mean ± s.e.m.

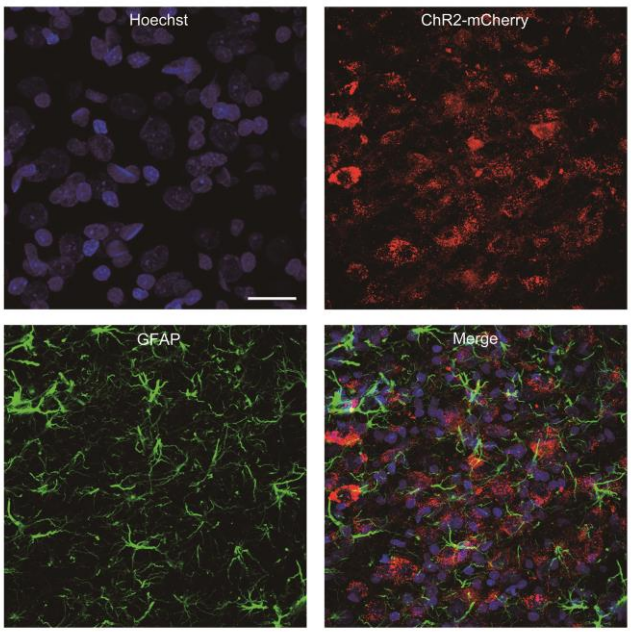

Supplementary Figure 18. GFAP- and ChR2-mCherry-expressing cells did not overlap significantly. High-magnification view reveals membrane localization of ChR2-mCherry. No obvious overlap was detected between ChR2-mCherry-expressing neurons (red) and GFAP-expressing neurons (astrocytes, green). Scale bar, 20 μm.

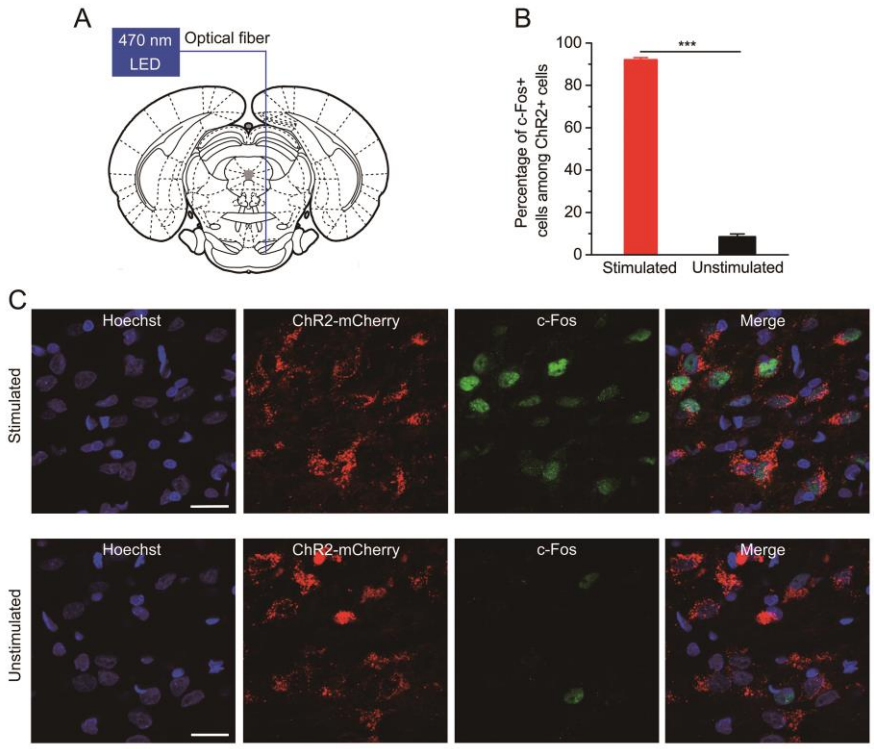

326

327 **Supplementary Figure 19.** 470-nm LED stimulation induced c-Fos expression in cells expressing
328 ChR2-mCherry in the right PN. (*A*) Schematic illustration of optical stimulation of
329 ChR2-mCherry-expressing cells in right PN. (*B–D*) Rats expressing ChR2-mCherry (red) in the
330 right PN were treated with or without 470-nm LED stimulation and the expression of c-Fos (green)
331 was examined. Representative magnification images of the right PN for the light stimulated group
332 (*C*) and unstimulated group (*D*) are shown. Scale bar, 20 μm. Quantification of c-Fos positive cells
333 among ChR2 positive cells is shown in (*B*).

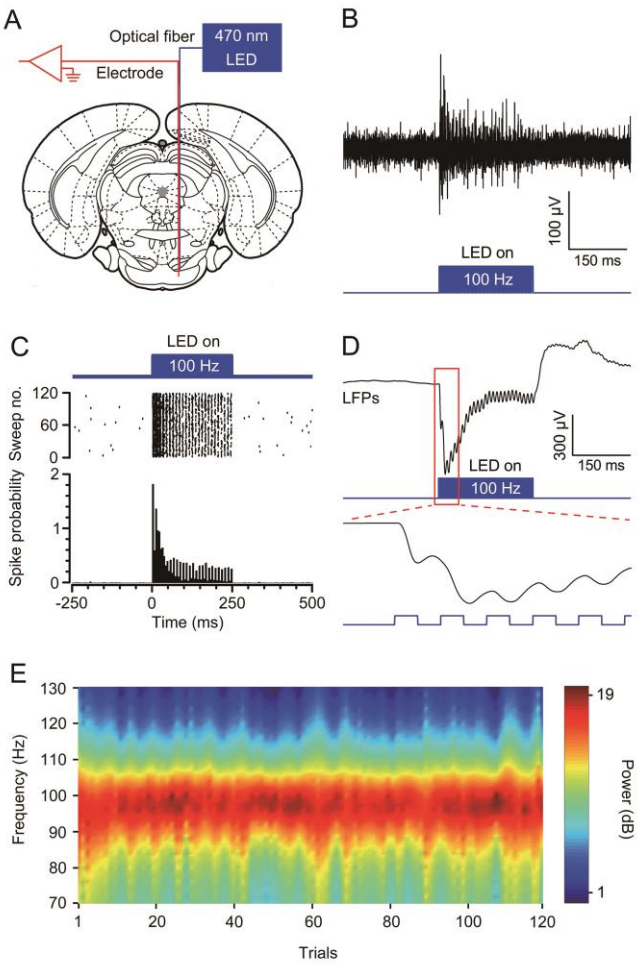

Supplementary Figure 20. 470-nm LED illumination evoked activation of ChR2-mCherry-expressing cells in the right PN. (*A*) Schematic showing *in vivo* optical stimulation and recording in the right PN. (*B*,*C*) Trains of 25 light pulses (470 nm, 15 mW/mm^2, 100 Hz, 5 ms pulse duration) induced reliable spikes in the right PN neurons recorded from head-fixed anesthetized rats injected with pAAV 2/9-hSyn-ChR2-mCherry. (*D*,*E*) Trains of 25 light pulses (470 nm, 15 mW/mm^2, 100 Hz, 5 ms pulse duration) also evoked robust LFP responses in the right PN in awake behaving rats. Note that the (*D*) graph illustrates an example of the mean value of 120 light-induced LFPs.

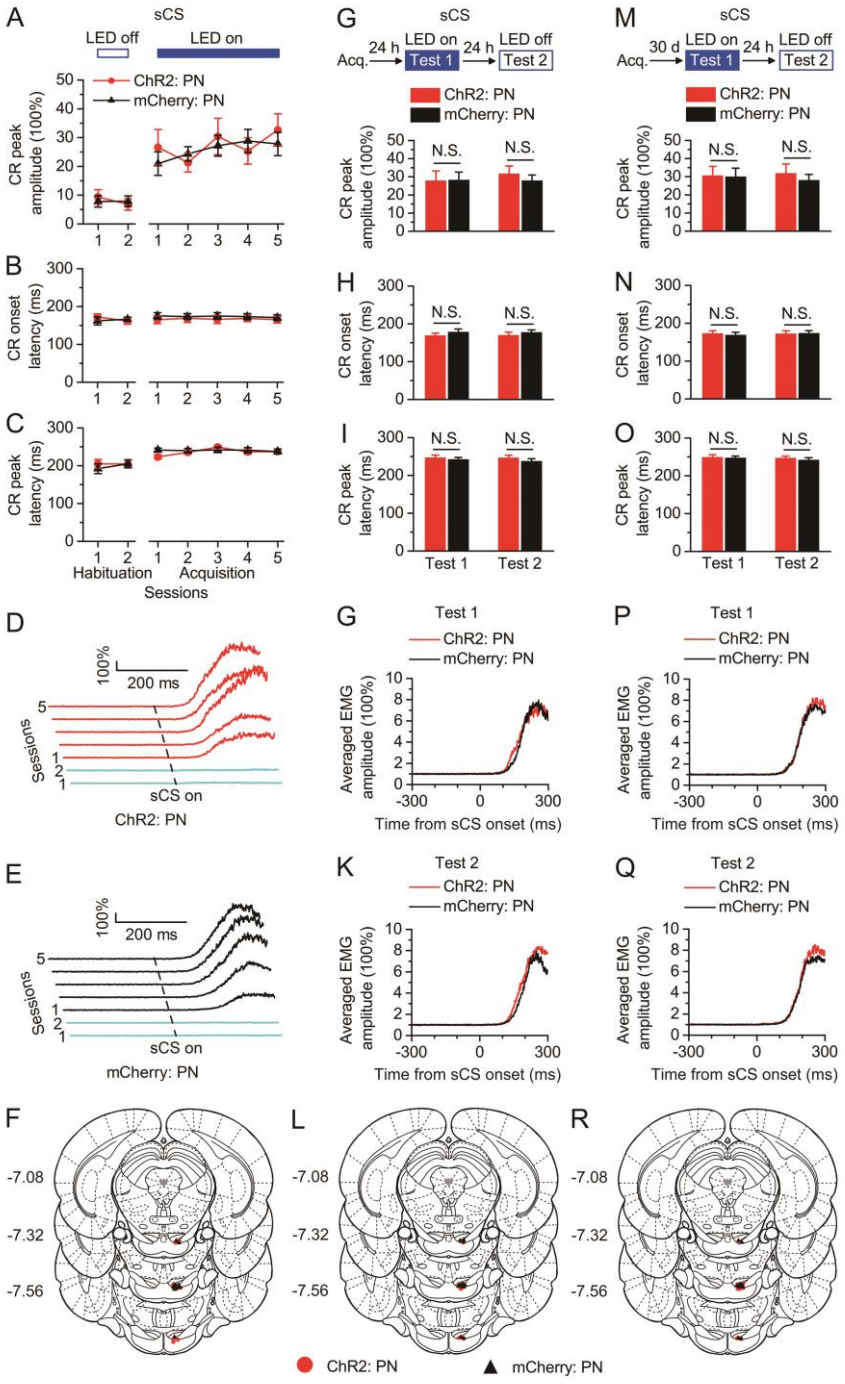

Supplementary Figure 21. Effects of optogenetic activation of the right PN on the peak amplitude, onset latency, and peak latency of CR with the sCS (related to Fig. 6*F–H*). (*A–C*) Top: Training and illumination protocol. Bottom: Optogenetic activation of the right PN during acquisition training failed to caused deficits in the peak amplitude (*A*), onset latency (*B*), or peak latency (*C*) of CR with the sCS (two-way ANOVA with repeated measures). (*D*,*E*) The EMG response topographies of ChR2: PN (*D*) and mCherry: PN (*E*) groups were shown across two habituation and five acquisition

sessions. (*F*) Approximate locations of optrode tips for optogenetic activation experiment (related to Fig. 6*F*) among rats of ChR2: PN and mCherry: PN groups. Numbers indicate the anteroposterior coordinates from bregma. (*G–I*) Top: Training and illumination protocol. Rats were eyeblink conditioned in the absence of optogenetic activation and tested 24 h later. Bottom: Twenty-four hours after the acquisition training, optogenetic activation of the right PN also did not affect the peak amplitude (*G*), onset latency (*H*), or peak latency (*I*) of CR with the sCS (N.S., not significant; two-tailed unpaired Student's t-test). (*J*,*K*) The EMG response topographies for ChR2: PN and mCherry: PN groups during test 1 (*J*) and test 2 (*K*) were shown. (*L*) Same as (*F*), except rats from the other optogenetic activation experiment (related to Fig. 6*G*). (*M–R*) Same as (*G–L*), except the optogenetic activation was applied at thirty days after the acquisition training (related to Fig. 6*H*; N.S., not significant; two-tailed unpaired Student's t-test). The EMG amplitude is given as a percentage of the baseline (100%) averaged EMG amplitude. Data are represented as mean ± s.e.m.

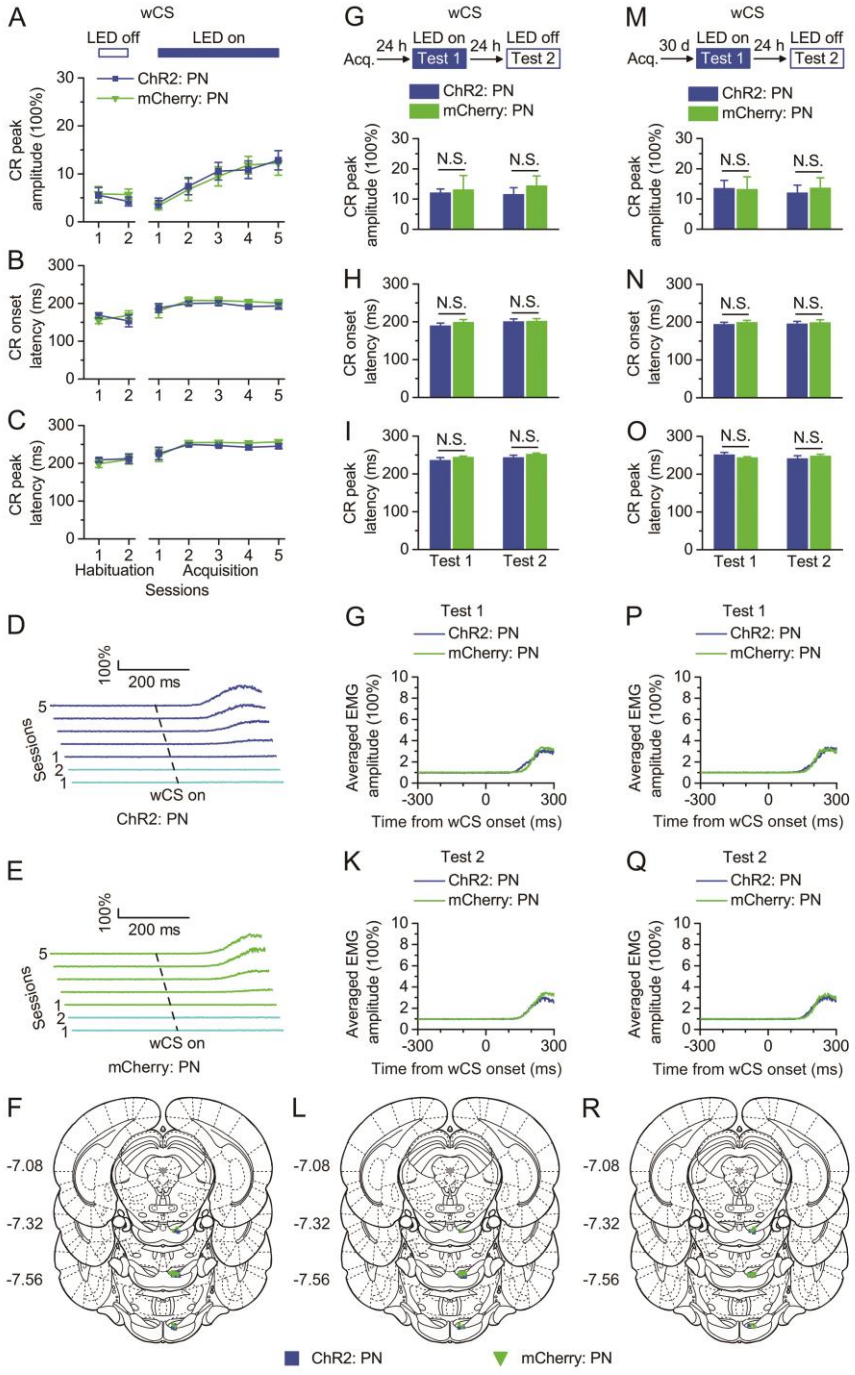

Supplementary Figure 22. Effects of optogenetic activation of the right PN on the peak amplitude, onset latency, and peak latency of CR with the wCS (related to Fig. 6*I–K*). (*A–F*) Top: Training and illumination protocol. Bottom: Optogenetic activation of the right PN during acquisition training failed to caused deficits in the peak amplitude (*A*), onset latency (*B*), or peak latency (*C*) of CR with the wCS (two-way ANOVA with repeated measures). (*D*,*E*) The EMG response topographies of ChR2: PN (*D*) and mCherry: PN (*E*) groups were shown across two habituation and five acquisition

sessions. (*F*) Approximate locations of optrode tips for optogenetic activation experiment (related to Fig. 6*I*) among rats of ChR2: PN and mCherry: PN groups. Numbers indicate the anteroposterior coordinates from bregma. (*G–I*) Top: Training and illumination protocol. Rats were eyeblink conditioned in the absence of optogenetic activation and tested 24 h later. Bottom: Twenty-four hours after the acquisition training, optogenetic activation of the right PN also did not affect the peak amplitude (*G*), onset latency (*H*), or peak latency (*I*) of CR with the wCS (N.S., not significant; two-tailed unpaired Student's t-test). (*J*,*K*) The EMG response topographies for ChR2: PN and mCherry: PN groups during test 1 (*J*) and test 2 (*K*) were shown. (*L*) Same as (*F*), except rats from the other optogenetic activation experiment (related to Fig. 6*J*). (*M–R*) Same as (*G–L*), except the optogenetic activation was applied at thirty days after the acquisition training (related to Fig. 6*K*; N.S., not significant; two-tailed unpaired Student's t-test). The EMG amplitude is given as a percentage of the baseline (100%) averaged EMG amplitude. Data are represented as mean ± s.e.m.